



Deposited via The University of Leeds.

White Rose Research Online URL for this paper:

<https://eprints.whiterose.ac.uk/id/eprint/4468/>

Article:

Merkin, J.H. (2008) The effect of the order of the autocatalysis on the transverse stability of reaction fronts. *The Journal of Chemical Physics*, 129 (3). Art. No. 034507. ISSN: 0021-9606

<https://doi.org/10.1063/1.2953313>

Reuse

See Attached

Takedown

If you consider content in White Rose Research Online to be in breach of UK law, please notify us by emailing eprints@whiterose.ac.uk including the URL of the record and the reason for the withdrawal request.

promoting access to White Rose research papers



Universities of Leeds, Sheffield and York
<http://eprints.whiterose.ac.uk/>

This is an author produced version of a paper published in **The Journal of Chemical Physics**.

White Rose Research Online URL for this paper:
<http://eprints.whiterose.ac.uk/4468/>

Published paper

Merkin, J.H. (2008) *The effect of the order of the autocatalysis on the transverse stability of reaction fronts*, The Journal of Chemical Physics, Volume 129 (3), 034507.

The effect of the order of the autocatalysis on the transverse stability of reaction fronts

J.H. Merkin

August 21, 2008

Department of Applied Mathematics
University of Leeds
Leeds, LS2 9JT, UK

Tel: +113 343 5108

FAX: +113 343 5090

Email: amtjhm@maths.leeds.ac.uk

Abstract

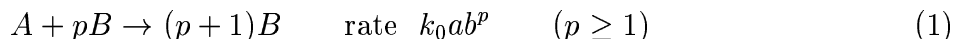
A linear stability analysis of planar reaction fronts to transverse perturbations is considered for a system based on an autocatalytic reaction of general order p . Dispersion curves, plots of the growth rate σ against a transverse wavenumber k , are obtained for a range of values of p and D , where D is the ratio of the diffusion coefficients of autocatalyst and substrate. A value D_0 of D , dependent on p , is found at which σ_{max} , the maximum value of σ in the unstable regime, is largest, with D_0 increasing as p is increased. An asymptotic analysis for small wavenumbers is derived which enables the region in the (p, D) parameter space for instability to be determined. An analysis for D small is undertaken which leads to upper bounds on the wavenumber for a possible instability.

Key words: autocatalytic reactions, reaction fronts, transverse instability.

1 Introduction

Planar reaction fronts that arise in models based on autocatalytic reactions can become transversely unstable if the diffusion coefficient of the autocatalyst is sufficiently different to that of the substrate. This has been established experimentally for the iodate-arsenous acid (IAA) system^{1,2} and for the chlorite-tetrathionate (CT) system³. Theoretical treatments of the IAA system have been mostly confined to using cubic autocatalytic kinetics, a good approximation in the arsenous acid excess case⁴. Using this reaction mechanism the condition for a transverse instability is that $D < D_c$, where $D_c \simeq 0.424$ ^{5,6} and where D is the ratio of the diffusion coefficients of autocatalyst and substrate.

In this paper we extend this discussion to an autocatalytic reaction of general order p , namely



where a and b are the concentrations of A and B respectively and k_0 is a constant. Cubic autocatalysis has $p = 2$. We limit our attention to the two spatial dimensions x and y , in part as we have in mind the experiments performed into the stability of reaction fronts in Hele-Shaw cells, see Refs. 7, 8 and 9 for example. These experiments have used both the IAA and CT reactions and start with the reactor being filled with the initial reactants, A in our model, at a uniform concentration. A small electric charge is applied in a thin strip across the reactor, locally initiating the reaction, producing some B in our model. Reaction-diffusion fronts propagate away from this initiation site, remaining planar if stable or developing ‘reaction fingers’ if diffusionally unstable.

The equations for our model are obtained using the standard thin-film approximation, with the concentrations being averaged over the gap width of the Hele-Shaw reactor. The resulting dimensionless equations for our model are then, see Refs. 10 and 11 for example,

$$\frac{\partial a}{\partial t} = \left(\frac{\partial^2 a}{\partial x^2} + \frac{\partial^2 a}{\partial y^2} \right) - ab^p, \quad \frac{\partial b}{\partial t} = D \left(\frac{\partial^2 a}{\partial x^2} + \frac{\partial^2 a}{\partial y^2} \right) + ab^p \quad (2)$$

where $D = D_B/D_A$. Eqs. (2) have been made dimensionless using a time scale $T_0 = (k_0 a_0^p)^{-1}$ and length scale $L_0 = (T_0 D_A)^{1/2}$, where a_0 is the initial uniform concentration of reactant A . Eqs. (2) have as a solution planar reaction fronts propagating with a constant speed c_0 in the x -direction. The y co-ordinate measures distance normal to this, i.e. along the reaction front. These planar reaction fronts can become longitudinally unstable if $D > 1$ and p is sufficiently large^{12,13} with the front initially losing stability through a Hopf bifurcation. The resulting simple oscillatory propagation of the front can have further instabilities leading to irregular or chaotic propagation. Here we are interested in possible transverse instabilities

and, as a consequence, we limit our attention to situations where $D < 1$.

We start by considering the planar reaction-diffusion fronts (traveling wave solutions) that Eqs. (2) can support, the base state for our stability analysis, for general values of p and D . $p = 1$ is a special case in that traveling wave solutions for which the boundary conditions ahead of the front are approached through exponentially small terms are possible for all $c_0 \geq 2\sqrt{D}$, see Ref. 14 for example. With $p > 1$ the requirement of exponential decay is sufficient to fix the wave speed uniquely, as established for cubic autocatalysis in Ref. 15. The singular way in which the $p = 1$ case is approached as $p \rightarrow 1$ from above is discussed in Ref. 16.

2 Traveling waves

Without any loss in generality we need consider only those waves propagating in the positive x -direction and to do so we introduce the traveling co-ordinate $\zeta = x - c_0 t$, where $c_0 (> 0)$ is the (constant) wave speed and then look for a solution in the form

$$a(x, y, t) = a(\zeta), \quad b(x, y, t) = b(\zeta) \quad (3)$$

The resulting traveling wave equations are

$$a'' + c_0 a' - ab^p = 0, \quad Db'' + c_0 b' + ab^p = 0 \quad (4)$$

on $-\infty < \zeta < \infty$ (where primes denote differentiation with respect to ζ), subject to the boundary conditions

$$a \rightarrow 1, b \rightarrow 0 \quad \text{as } \zeta \rightarrow \infty, \quad a \rightarrow 0, b \rightarrow 1 \quad \text{as } \zeta \rightarrow -\infty \quad (5)$$

The wave speed c_0 in general depends on both D and p and has to be determined numerically. To fix the wave speed uniquely we need to assume the boundary conditions as $\zeta \rightarrow \infty$ are approached through exponentially small terms^{10,17}. This assumption is built into the numerical integrations.

An asymptotic analysis for p large is given in Refs. 12 and 13, the result is that

$$c_0 \sim \sqrt{2} D p^{-1} + \dots \quad \text{as } p \rightarrow \infty \quad (6)$$

Graphs of c_0 against p are shown in Fig. 1, the asymptotic forms given by (6) are shown by broken lines. This figure shows that, for a given value of p , the wave speed decreases as D is decreased in line with the results for cubic autocatalysis given in Refs. 6 and 10. For a given

value of D , the wave speed also decreases as p is increased, with the asymptotic expression (6) for p large giving a good approximation for c_0 even at moderate values of p .

We can determine how the wave speed varies with p when D is small following the treatment for the case with $p = 2$ given in Ref. 10. There is an inner region in which ζ and b are left unscaled and in which

$$a = D\bar{a}, \quad c = D\bar{c}, \quad \text{with } \bar{a}, \bar{c} \text{ of } O(1) \text{ as } D \rightarrow 0 \quad (7)$$

An expansion in powers of D gives the leading-order problem

$$\bar{a}'' - \bar{a}b^p = 0, \quad b'' + \bar{c}_0 b' + \bar{a}b^p = 0 \quad (8)$$

subject to

$$\bar{a} \rightarrow 0, \quad b \rightarrow 1 \quad \text{as } \zeta \rightarrow -\infty, \quad \bar{a} \sim \bar{c}_0 \zeta, \quad b \rightarrow 0 \quad \text{as } \zeta \rightarrow \infty \quad (9)$$

Eqs. (8, 9) have to be solved numerically and the resulting leading-order wave speed \bar{c}_0 is plotted against p in Fig. 2. From (6), $\bar{c}_0 \sim \sqrt{2}p^{-1}$ for p large and this is shown in Fig. 2 by a broken line. This figure shows, as perhaps expected from Fig. 1, that \bar{c}_0 decreases as p is increased. There is also good agreement with asymptotic form for \bar{c}_0 for p large. To complete the solution an outer region is required in which b is exponentially small and $\bar{\zeta} = D\zeta$. The leading-order problem gives $a = 1 - e^{-\bar{c}_0 \bar{\zeta}}$ which has $a \rightarrow 1$ as $\bar{\zeta} \rightarrow \infty$ and matches with the inner region.

3 Stability analysis

To discuss the diffusional stability of the reaction fronts given by (4, 5), we put

$$a(\zeta, y, t) = a(\zeta) + e^{\sigma t + iky} A(\zeta), \quad b(\zeta, y, t) = b(\zeta) + e^{\sigma t + iky} B(\zeta) \quad (10)$$

where $a(\zeta)$ and $b(\zeta)$ are the traveling wave solutions given by (4, 5) and where A, B are small perturbations. We substitute (10) into Eqs. (2), written in terms of the travelling co-ordinate ζ , linearizing the resulting equations. This leads to an eigenvalue problem for $A(\zeta), B(\zeta)$ in terms of the growth rate σ and the wavenumber k as

$$A'' + c_0 A' - (b^p + k^2 + \sigma)A - p a b^{p-1} B = 0 \quad (11)$$

$$DB'' + c_0 B' - (Dk^2 - p a b^{p-1} + \sigma)B + b^p A = 0 \quad (12)$$

where primes still denote differentiation with respect to ζ , subject to the boundary conditions that

$$A \rightarrow 0, \quad B \rightarrow 0, \quad \text{as } \zeta \rightarrow \pm\infty \quad (13)$$

Dispersion curves, plots of σ against k for given values of p and D , were obtained by solving equations (11, 12) numerically by a shooting method. This approach required the solution to the traveling wave equations and built in the asymptotic forms for the solution as $\zeta \rightarrow \pm\infty$ resulting from (5) and (13). One of the arbitrary constants that arises in this process being put to unity to force a non-trivial solution. The resulting linear boundary-value problem was solved using a standard shooting method (D02AGF in the NAG library). This method converged readily. A similar method was also used to solve the traveling wave problem (4, 5).

In Fig. 3(a) we give dispersion curves for $D = 0.3$ and a range of values of p . This figure shows that the system becomes more unstable (larger positive values of σ) as p is increased from $p = 2$ to $p = 3$. For the higher values of p , the system then becomes more stable, i.e. smaller positive values of σ and a smaller range of unstable wavenumbers. The maximum value σ_{max} of σ obtained from these (and related) dispersion curves is plotted against p in Fig. 3(b). (In this and subsequent figures \bullet corresponds to values of parameters used for the numerical integrations.) This figure indicates that σ_{max} achieves its greatest value at $p \simeq 3.0$ for this value of D . The system remains unstable for all values of p greater than this, though the positive growth rates σ become smaller for the larger values of p . For this case the system is stable ($\sigma < 0$ for all k) for $p = 1.4$. With $p = 1.45$ the system becomes unstable though with a very small value for σ_{max} and a very small range of unstable wavenumbers.

In Fig. 4(a) we plot dispersion curves for $D = 0.6$. In this case for $p = 2$, $D_c = 0.424$ and the system is stable^{5,6} as can be seen in the figure. The system is also stable with $p = 3$ in this case and becomes unstable when $p = 4$ with increasingly larger positive values of σ as p is increased. The corresponding values of σ_{max} are shown in Fig. 4(b). This latter figure shows that the system has a transition to instability at $p \simeq 3.5$ and is then unstable for values of p greater than this. The values of σ_{max} have a maximum at $p \simeq 8.5$ and then decrease very slowly as p is increased further.

In Ref. 6 we noted that, for cubic autocatalysis ($p = 2$), the growth rates achieved a maximum at $D = D_0 \simeq 0.16$ and decreased for smaller values of D . The same behaviour, perhaps not unexpectedly, is seen in the present case as is illustrated in Fig. 5 where we plot σ_{max} against D for different values of p . This figure shows that the value of D_0 , where σ_{max} achieves a maximum value, increases as p is increased as well as the range of D where the system is unstable. However the figure also indicates that the maximum value of σ_{max}

decreases as p is increased.

Figs. 3(b), 4(b) and 5 indicate that the stability of the system depends on both p and D (as might be expected) with there being a critical value $D_c = D_c(p)$ of D at which the system changes stability from being fully stable, $D > D_c(p)$, to having a range of unstable wavenumbers, $D < D_c(p)$. We can gain further information about how D_c varies with p by considering the solution to Eqs. (11, 12) for k small, following closely the treatment given in Ref. 6 for the case when $p = 2$. We note that, for $D = 1$, $\sigma = -k^2$ and hence we can take $D < 1$.

3.1 Solution for small wavenumbers, k

We look for a solution to equations (11, 12) (for $D \neq 1$) valid for k small by expanding

$$\begin{aligned} A(\zeta; k) &= A_0(\zeta) + k^2 A_1(\zeta) + \dots, \\ B(\zeta; k) &= B_0(\zeta) + k^2 B_1(\zeta) + \dots, \\ \sigma(k) &= \sigma_0 k^2 + \sigma_1 k^4 \dots \end{aligned} \tag{14}$$

It is easily seen that the solution to the leading-order problem is

$$A_0 = a'(\zeta), \quad B_0 = b'(\zeta) \tag{15}$$

where $a(\zeta)$, $b(\zeta)$ are the traveling wave solutions given by (4, 5). Expression (15) reflects the fact that the traveling wave equations (4) are translationally invariant. Any arbitrary multiple of (15) is also a solution to the leading-order problem and, without any loss in generality, we can take this multiple to be unity.

At $O(k^2)$ we obtain, using (15),

$$A_1'' + c_0 A_1' - b^p A_1 - p a b^{p-1} B_1 = (\sigma_0 + 1) a' \tag{16}$$

$$D B_1'' + c_0 B_1' + p a b^{p-1} B_1 + b^p A_1 = (\sigma_0 + D) b'$$

subject to the boundary conditions

$$A_1, B_1 \rightarrow 0 \quad \text{as } \zeta \rightarrow \pm\infty \tag{17}$$

We note that $A_1 = a'$, $B_1 = b'$ is a solution to the homogeneous problem satisfying the homogeneous boundary conditions (17). Thus a compatibility condition is required for the non-homogeneous problem (16) to have a solution which also satisfies all the required boundary conditions. It is this condition that determines the constant σ_0 . To derive this condition

we first need to derive the corresponding adjoint problem $U(\zeta)$, $V(\zeta)$. To do this we follow Ref. 6 directly to obtain

$$\frac{d}{d\zeta} (e^{c_0\zeta}U') - b^p(e^{c_0\zeta}U - e^{c_0\zeta/D}V) = 0 \quad (18)$$

$$\frac{d}{d\zeta} (De^{c_0\zeta/D}V') - pab^{p-1}(e^{c_0\zeta}U - e^{c_0\zeta/D}V) = 0$$

The compatibility condition is then, again from Ref. 6, that

$$(\sigma_0 + 1) \int_{-\infty}^{\infty} e^{c_0\zeta} a' U d\zeta + (\sigma_0 + D) \int_{-\infty}^{\infty} e^{c_0\zeta/D} b' V d\zeta = 0 \quad (19)$$

It is condition (19) that then determines σ_0 .

The adjoint problem (18) has to be solved numerically and this was done by applying the same shooting method that was used to calculate the dispersion curves, as given by (11 – 13). Having calculated U and V , these were then used to calculate the integrals in (19) to determine σ_0 . Graphs of σ_0 against D are shown in Fig. 6(a) for a range of values of p . Fig. 6(a) shows that σ_0 achieves similar maximum values for $p = 2$ and for $p = 4$, though for $p = 4$ the system is unstable, $\sigma_0 > 0$, for a greater range of D . By $p = 6$ the maximum value of σ_0 is becoming smaller. This point is more clearly seen in Fig. 6(b), where we plot $\sigma_{0,max}$ against p . From this figure we see that $\sigma_{0,max}$ has a maximum value at $p \simeq 3.0$ and then decreases as p is increased.

One point to note from the curves plotted in Fig. 6(a) is that there is a value D_c of D at which σ_0 passes through zero. We calculated the value of D_c more accurately by refining the increment in D around the expected value of D_c , for a given value of p , and the corresponding results are shown in Fig. 7 with a plot of D_c against p . For $D > D_c(p)$, $\sigma_0 < 0$ and, since the the dispersion curves in the unstable regimes seem to have a ‘parabolic’ appearance, as in Figs. 3(a) and 4(a), we can expect the system to be stable in this case. For $D < D_c(p)$, $\sigma_0 > 0$ and there will be a range of wavenumbers over which $\sigma > 0$ and the system will be unstable. These regions of stability and instability are labelled on Fig. 7. Fig. 7 shows that D_c increases as p is increased. From Ref. 13 we could expect that $D_c \rightarrow 1$ from below as $p \rightarrow \infty$, though by $p = 10$, $D_c = 0.736$ and is increasing only very slowly at this value of p . This suggests that very large values of p might be required for the large p asymptotic limit derived in Ref. 13 to be achieved with some degree of accuracy. Though the range of D where the system is unstable increases with p , we see from Fig. 6(b) that $\sigma_{0,max}$ decreases, so we can expect for the general dispersion curves that σ_{max} will also decrease for the larger values of p , as is borne out in Figs. 3(b), 4(b) and 5.

The question remains as to whether the system can be unstable for all $p > 1$ or whether there is some critical value of p strictly greater than one that is required for a possible instability, i.e. does $D_c \rightarrow 0$ as $p \rightarrow 1$ from above or is there some value p_c of p , with $p_c > 1$, at which $D_c = 0$? To discuss this point further we obtain a solution of equations (11, 12) valid for D small.

3.2 Solution for D small

The nature of the solution of the traveling waves for D small is described in detail in Ref. 10 for $p = 2$ and summarized for general values of $p > 1$ by equations (7 – 9) and Fig. 2(b). Motivated by (7) and the solution for $p = 2$ given in Ref. 6, we put

$$A = D \bar{A}, \quad \sigma = D \bar{\sigma} \quad (20)$$

with the eigenvalue problem in the inner region becoming at leading order on using (7)

$$\bar{A}'' - (b^p + k^2) \bar{A} - p \bar{a} b^{p-1} B = 0 \quad (21)$$

$$B'' + \bar{c}_0 B' - (k^2 - p \bar{a} b^{p-1} + \bar{\sigma}) B + b^p \bar{A} = 0 \quad (22)$$

Equations (21, 22) were solved numerically using the same shooting method technique described previously for finding the dispersion curves. The results are shown in Fig. 8(a) with plots of $\bar{\sigma}$ against k for different values of p . This figure shows that $\bar{\sigma}_{max}$ and the range of unstable wavenumbers decrease as the value of p is increased. This is brought out more clearly in Fig. 8(b), where we plot $\bar{\sigma}_{max}$ against p . This figure also shows that $\bar{\sigma}_{max}$ increases rapidly as p is decreased from $p = 2$. As was mentioned in Ref. 6 for the case $p = 2$, the range of unstable wavenumbers increase as D is decreased and k_{max} , the maximum value of k where $\bar{\sigma} > 0$ in the solution for D small can act as an upper bound for the range of unstable wavenumbers for the larger values of D . We plot k_{max} against p in Fig. 8(c), showing that the values of k_{max} decrease as p is increased (in line with Fig. 8(a)) and gives an increasingly larger range of unstable wavenumbers as p is decreased towards $p = 1$.

We can gain further insight into how $\bar{\sigma}$ varies with p by looking for a solution of equations (21, 22) for k small. We have to include terms of $O(k)$ in the expansion, the reason for this will become clear below. We now expand

$$\bar{A} = \bar{A}_0 + k \bar{A}_1 + k^2 \bar{A}_2 + \dots, \quad B = \bar{B}_0 + k \bar{B}_1 + k^2 \bar{B}_2 + \dots, \quad \bar{\sigma} = k \bar{\sigma}_0 + k^2 \bar{\sigma}_1 + \dots \quad (23)$$

Note that $\bar{\sigma}$ is $O(k)$ for small k , not $O(k^2)$ as previously taken in (14). This will be required in this asymptotic development and is also suggested by the dispersion curves shown in Fig.

8(a). The leading-order solution is again

$$\bar{A}_0 = \bar{a}', \quad \bar{B}_0 = b' \quad (24)$$

where \bar{a}, b are the solutions to (8, 9). We note that

$$\bar{A}_0 \rightarrow \bar{c}_0, \quad \bar{B}_0 \rightarrow 0 \quad \text{as } \zeta \rightarrow \infty, \quad \bar{A}_0, \bar{B}_0 \rightarrow 0 \quad \text{as } \zeta \rightarrow -\infty \quad (25)$$

where \bar{c}_0 depends on p , as shown in Fig. 2.

At $O(k)$ we obtain

$$\bar{A}_1'' - b^p \bar{A}_1 - p \bar{a} b^{p-1} \bar{B}_1 = 0 \quad (26)$$

$$\bar{B}_1'' + \bar{c}_0 \bar{B}_1' + p \bar{a} b^{p-1} \bar{B}_1 + b^p \bar{A}_1 = \bar{\sigma}_0 b'$$

Equations (26) have the solution

$$\bar{A}_1 = -\frac{\bar{\sigma}_0}{\bar{c}_0} \left(\zeta \bar{a}' + \frac{2}{p} \bar{a} \right) + \alpha_1 \bar{a}', \quad \bar{B}_1 = -\frac{\bar{\sigma}_0}{\bar{c}_0} \left(\zeta b' + \frac{2}{p} b \right) + \alpha_1 b' \quad (27)$$

for some constant α_1 . From (27)

$$\bar{A}_1 \sim -\frac{\bar{\sigma}_0(p+2)}{p} \zeta + \dots, \quad \bar{B}_1 \rightarrow 0 \quad \text{as } \zeta \rightarrow \infty, \quad \bar{A}_1 \rightarrow 0, \quad \bar{B}_1 \rightarrow -\frac{2\bar{\sigma}_0}{\bar{c}_0 p} \quad \text{as } \zeta \rightarrow -\infty \quad (28)$$

From (25) and (28) we see that the outer boundary conditions are not satisfied. Hence this must be an inner region with outer regions being required, one for $\zeta > 0$ and one for $\zeta < 0$.

In both these outer regions the independent variable is $Y = k \zeta$.

We consider the outer solution for $\zeta > 0$ first. In this region

$$b, B \equiv 0, \quad \bar{A}'' - \bar{A} = 0 \quad (29)$$

where primes now denote differentiation with respect to Y , subject to, from (25, 28),

$$\bar{A} \sim \bar{c}_0 \left(1 - \frac{\bar{\sigma}_0(p+2)}{\bar{c}_0 p} Y + \dots \right) + \dots \quad \text{as } Y \rightarrow 0, \quad \bar{A} \rightarrow 0 \quad \text{as } Y \rightarrow \infty \quad (30)$$

An expansion

$$\bar{A} = \tilde{A}_0 + k \tilde{A}_1 + \dots \quad (31)$$

gives at leading order

$$\tilde{A}_0 = \bar{c}_0 e^{-Y} \quad (32)$$

The form of the solution in this outer region (and the one in the outer region for $\zeta < 0$) is the reason that expansion (23) was in powers of k . Applying the matching condition (30) then gives

$$\bar{\sigma}_0 = \frac{\bar{c}_0 p}{p+2} \quad (33)$$

We note that, in (33), \bar{c}_0 depends on p (as shown in Fig. 2) and a graph of $\bar{\sigma}_0$ against p is given in Fig. 9. The asymptotic form for p large that $\bar{\sigma}_0 \sim \sqrt{2}p^{-1}$ is shown by the broken line and gives good agreement with the numerically determined values even at moderate values of p . This figure indicates that $\bar{\sigma}_0$ decreases as p increases, consistent with Figs. 6(a), 8(a) and 8(b) and the dispersion curves shown in Figs. 3(a), 4(a) and 6(a). The values of $\bar{\sigma}_0$ increase rapidly as p is reduced towards $p = 1$. Expression (33) holds for all $p > 1$, noting that the asymptotic behaviour of the traveling wave equations for D small is different to that given by (7) when $p = 1^{10}$ suggesting a singular limit as $p \rightarrow 1$ from above, as is the case for $D = 1^{16}$. Though our results are not strictly applicable when $(p - 1)$ is small, however they do suggest the possibility of a transverse instability for all $p > 1$ provided that D is sufficiently small.

The outer region for $\zeta < 0$ follows in a similar way, here

$$\bar{a}, \bar{A} \equiv 0, \quad \text{and} \quad B = k \tilde{B} \quad (34)$$

giving

$$\bar{c}_0 \tilde{B}' - (\bar{\sigma}_0 + k \bar{\sigma}_1 + \dots) \tilde{B} + k(\tilde{B}'' - \tilde{B}) = 0 \quad (35)$$

An expansion in powers of k then gives, for the leading-order term \tilde{B}_0 subject to, from (25, 28),

$$\tilde{B}_0 \sim -\frac{2\bar{\sigma}_0}{p\bar{c}_0} + \dots \quad \text{as } Y \rightarrow 0, \quad \tilde{B}_0 \rightarrow 0 \quad \text{as } Y \rightarrow -\infty \quad (36)$$

that

$$\tilde{B}_0 = -\frac{2\bar{\sigma}_0}{p\bar{c}_0} \exp\left(\frac{\bar{\sigma}_0 Y}{\bar{c}_0}\right) \quad (37)$$

4 Conclusions

We have considered how the order p of a simple autocatalytic reaction scheme (1) affects the transverse stability of the planar reaction fronts generated by this mechanism. Our main conclusion is that the higher the order of the autocatalysis, the larger the range of $D = D_B/D_A$ over which the reaction fronts are unstable, see Figs. 5 and 6(a) and being summarized in Fig 7. However, for these larger reaction orders the (linear) growth rates σ decrease as the reaction order p is increased, see Figs. 3(b) and 4(b). This has the effect

of increasing the time scales over which the regular cellular patterns or more incoherent structures seen in diffusion-driven instabilities of reaction fronts will appear, see Refs. 1, 5 and 18 for example. As noted previously for cubic autocatalysis⁶, there is an ‘optimum’ value D_0 of D which gives the fastest (linear) growth rate. The same feature is seen for a general autocatalytic order, with the value of D_0 increasing with increasing p , as seen in Fig. 5.

The analysis to determine the nature of the dispersion curves for small wavenumbers k is a useful guide to the overall stability of the system. This gives $\sigma \sim \sigma_0 k^2$ for k small and clearly, if $\sigma_0 > 0$, then there must be some range of wavenumbers over which $\sigma > 0$ and the system is unstable. Moreover, since the dispersion curves for unstable systems have a ‘parabolic’ appearance, this analysis can also indicate, when $\sigma_0 < 0$, when the system is fully stable. As seen previously for cubic autocatalysis⁶, the range of unstable wavenumbers increases as D is reduced from its bifurcation value D_c . The same effect is also seen in the present case and thus the values of $k_{max}(p)$ obtained from asymptotic analysis for D small, see Fig. 8(c), with the system being stable for $0 < k < k_{max}$ in this limit, give an upper bound on the range of possible unstable wavenumbers in the general case when $D < D_c(p)$. Hence a necessary condition for reaction system of with L to be unstable is that $L > 2\pi/k_{max}$.

Our results assumed that $p > 1$ and we considered the question as to whether a system given by reaction (1) could be unstable for all $p > 1$. Our numerical results strongly indicate that D_c decreases as p is reduced, see particularly Fig. 5, with $D_c \rightarrow 0$ as $p \rightarrow 1$ (from above) being suggested. This was, in part, a motivation for considering the small D analysis and our results, see expression (33) and Fig. 9, also suggest that an instability is possible for all $p > 1$ provided that D is sufficiently small. The growth rates also increase quite markedly as p is reduced towards unity (Figs. 5 and 8(a), 8(b)) perhaps indicating a singular limit as $p \rightarrow 1$ (and $D \rightarrow 0$). This would not be surprising and could well be expected as the $p = 1$ case is a singular limit for the reaction-diffusion fronts¹⁶, the base state for any stability analysis. It has been established¹⁹ that the large time behaviour for reaction systems (1) with $p < 1$ is qualitatively different, in this case reaction fronts do not develop and the system approaches the fully reacted state uniformly at large times, again suggesting a singular limit as $p \rightarrow 1$.

References

- ¹D. Horváth and K. Showalter. *J. Chem. Phys.* **102**, 2471 (1995).
- ²D. Horváth and A. Tóth. *J. Chem. Phys.* **108**, 1447 (1998).
- ³M. Fuentes, M.N. Kuperman and P. De Kepper. *J. Phys. Chem. A* **105**, 6769 (2001).
- ⁴J.H. Merkin and H. Ševčíková. *Phys. Chem. Chem. Phys.* **1**, 91 (1999).
- ⁵A. Malevanets, A. Careta and R. Kapral. *Phys. Rev. E* **52**, 4724 (1995).
- ⁶J.H. Merkin and I.Z. Kiss. *Phys. Rev. E* **72**, 026219 (2005).
- ⁷M. Böckmann and S.C. Müller. *Phys. Rev. Letters* **85**, 2506 (2000).
- ⁸D. Horváth, T. Bánsági Jr. and Á. Tóth. *J. Chem. Phys.* **117**, 4399 (2002).
- ⁹A. Zdražil and H. Ševčíková. *J. Chem. Phys.* **123**, 174509 (2005).
- ¹⁰J. Billingham and D.J. Needham. *Phil. Trans. R. Soc. Lond.* **A334**, 1 (1991).
- ¹¹D.J. Needham and J.H. Merkin. *Nonlinearity* **5**, 413 (1992).
- ¹²M.J. Metcalf, J.H. Merkin and S.K. Scott. *Proc. R. Soc. Lond.* **A447**, 155 (1994).
- ¹³N.J. Balmforth, R.V. Craster and S.J.A. Malham. *Proc. R. Soc. Lond.* **A455**, 1401 (1999).
- ¹⁴J.A. Leach and D.J. Needham. *Matched asymptotic expansions in reaction-diffusion theory*. Springer, London, 2004.
- ¹⁵J. Billingham and D.J. Needham. *Dynamics and Stability of Systems* **6**, 33 (1991).
- ¹⁶J.H. Merkin and D.J. Needham. *Z. angew Math. Phys. (ZAMP)* **44**, 707 (1993).

¹⁷J. Billingham and D.J. Needham. *Quart. Appl. Math.* **50**, 343 (1992).

¹⁸D. Horvath, V. Petrov, S.K. Scott and K. Showalter. *J. Chem. Phys.* **98**, 6332 (1993).

¹⁹A.C. King and D.J. Needham. *Proc. R. Soc. Lond.* **A437**, 657 (1992).

Captions for figures

Figure 1. Plots of the wave speed c_0 against p for $D = 1.0, 0.5, 0.2$. The asymptotic result for p large (6) is shown by the broken lines.

Figure 2. A plot of the wave speed \bar{c}_0 against p for small D obtained from (8, 9). The asymptotic result for p large is shown by a broken line.

Figure 3. (a) dispersion curves, plots of σ against k , obtained from solving (11 – 13) numerically with $D = 0.3$ and $p = 2, 3, 5, 7$. (b) a plot of σ_{max} against p for $D = 0.3$.

Figure 4. (a) dispersion curves, plots of σ against k , obtained from solving (11 – 13) numerically with $D = 0.6$ and $p = 2, 4, 6, 8, 10$. (b) a plot of σ_{max} against p for $D = 0.6$.

Figure 5. A plot of σ_{max} against D for $p = 1.5, 2, 3, 5$ to illustrate that σ_{max} achieves a maximum value at a finite value D_0 of D .

Figure 6. (a) graphs of σ_0 against D for $p = 2, 4, 6$ calculated from the compatibility condition (19) for the small wavenumber analysis. Note that $\sigma \sim \sigma_0 k^2 + \dots$ for k small. (b) the variation of $\sigma_{0,max}$ with p .

Figure 7. The values D_c where $\sigma_0 = 0$, from the small wavenumber analysis, plotted against p . The regions where the system is stable and unstable are labelled on the figure.

Figure 8. (a) graphs of $\bar{\sigma}$ against k for $p = 1.5, 2, 3, 5, 8$ obtained from the solution for small D (21, 22). (b) a plot of $\bar{\sigma}_{max}$ against p . (c) values of k_{max} , the maximum value of k for which $\bar{\sigma} > 0$, plotted against p .

Figure 9. A plot of $\bar{\sigma}_0$ given by (34), the asymptotic form $\bar{\sigma}_0 \sim \sqrt{2} p^{-1}$ is shown by the broken line.

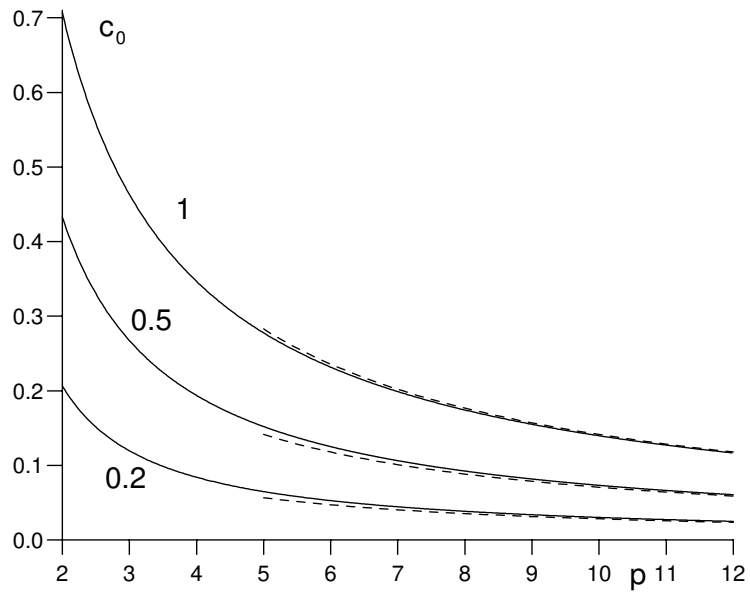


Figure 1

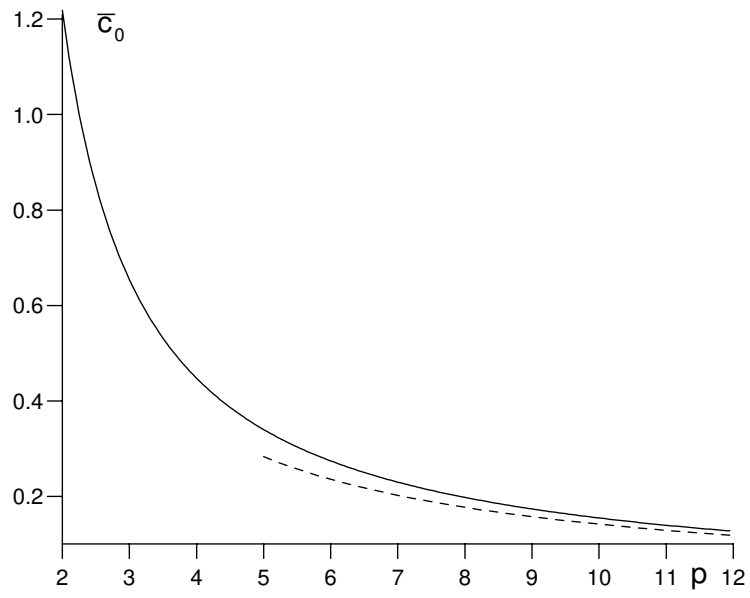


Figure 2

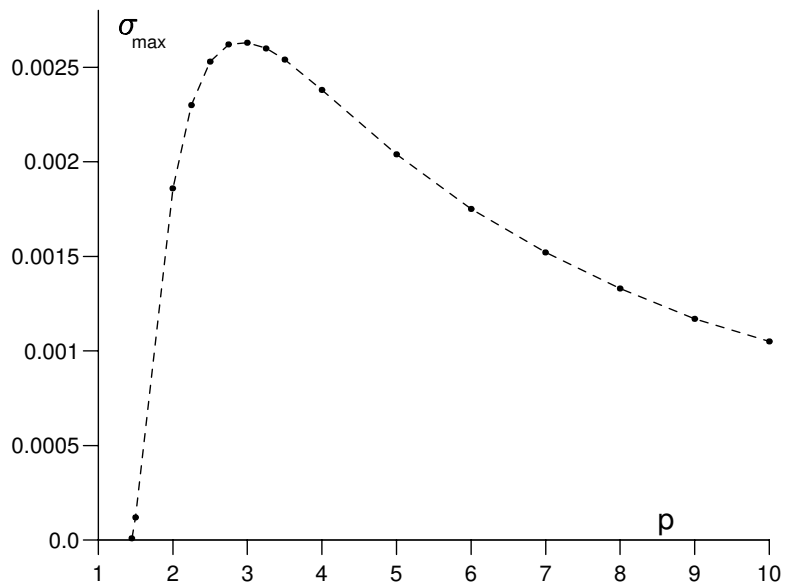
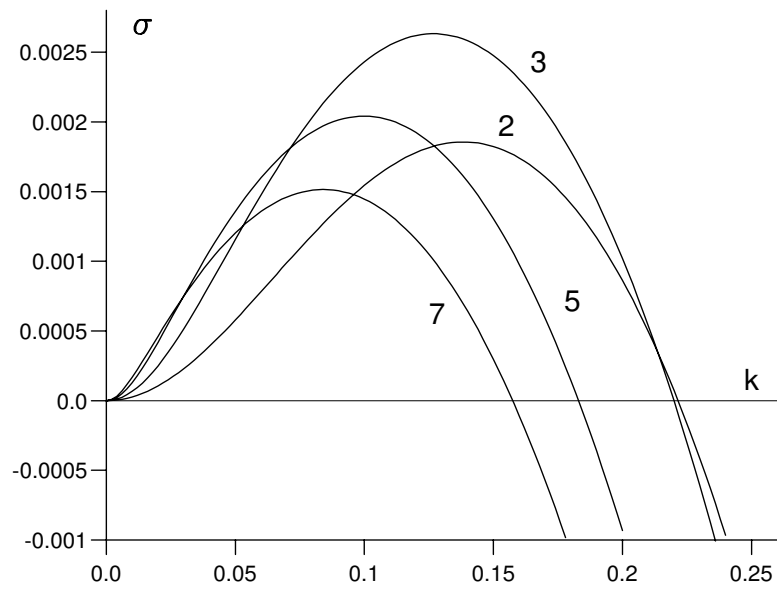


Figure 3

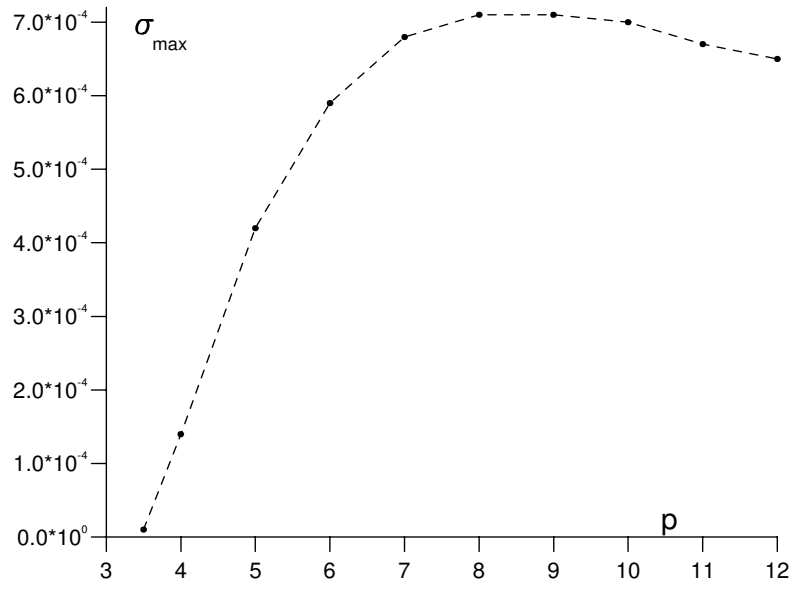
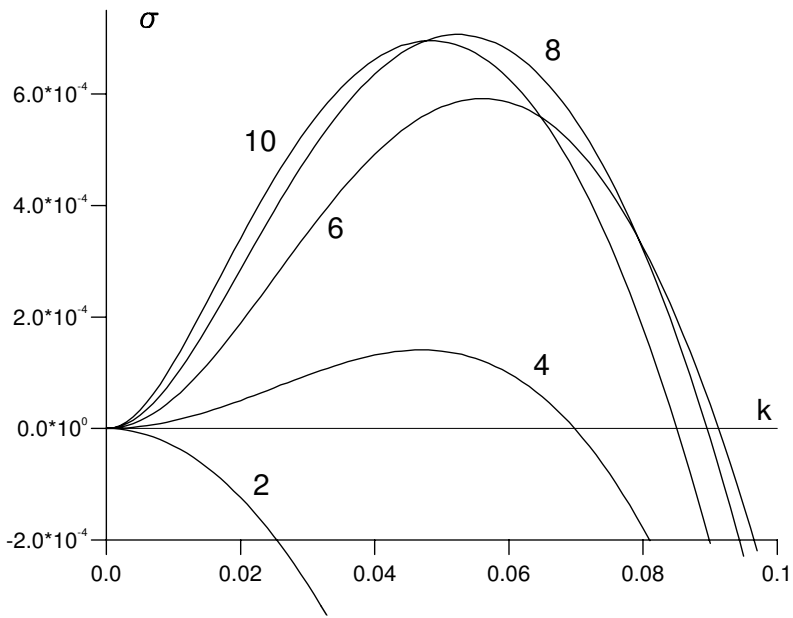


Figure 4

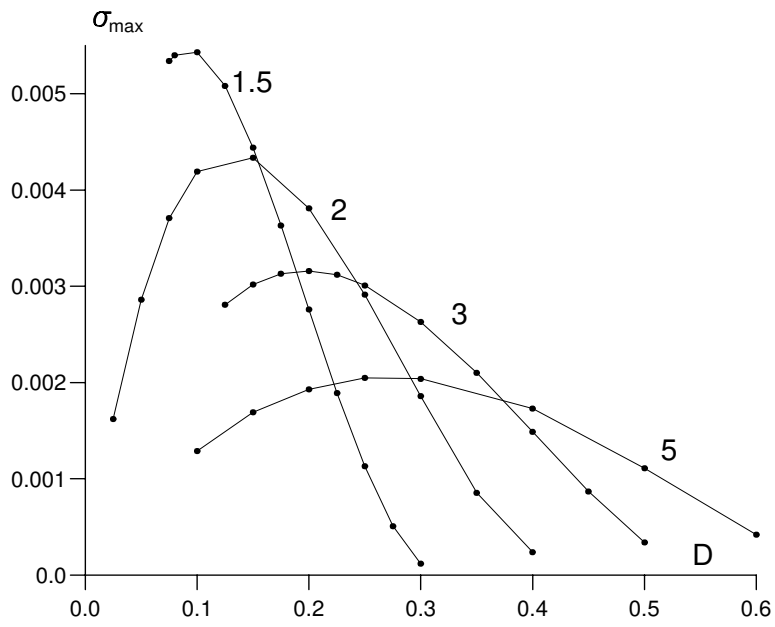


Figure 5

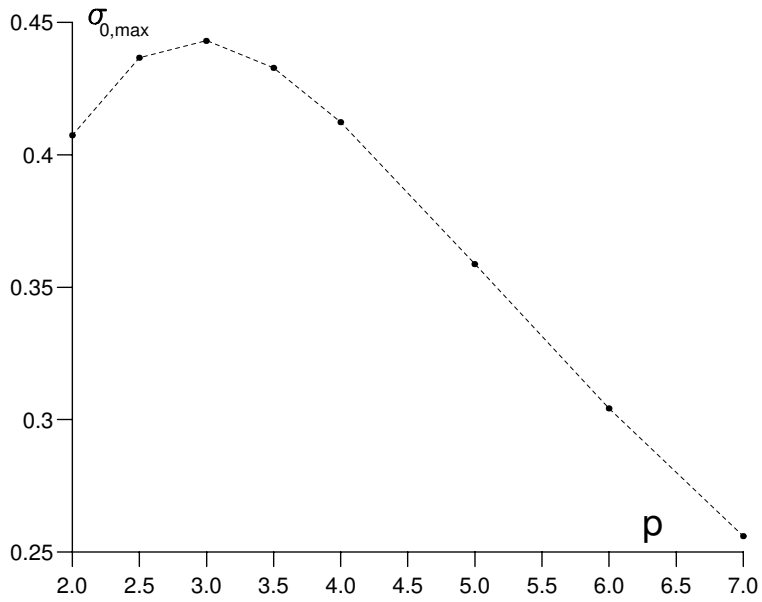
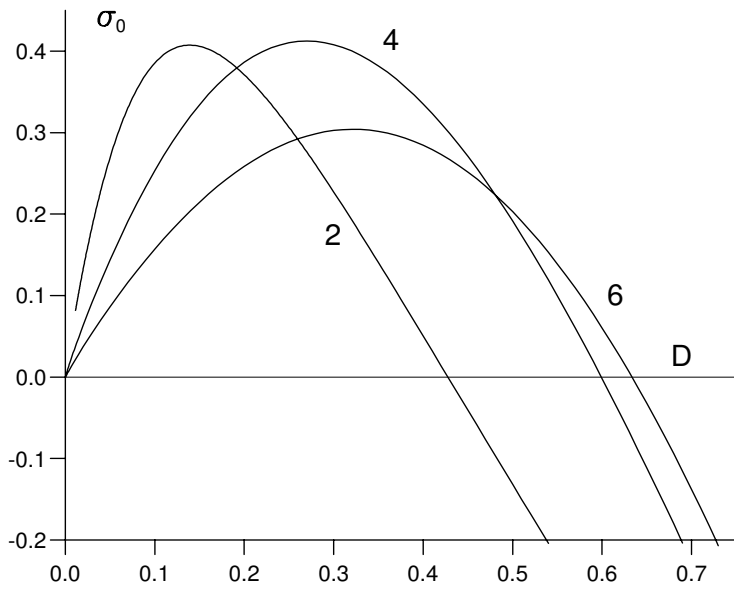


Figure 6

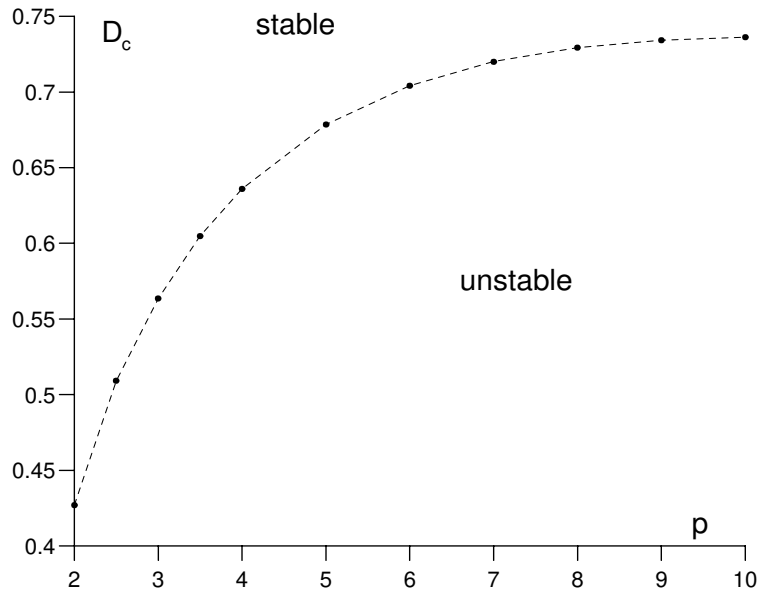


Figure 7

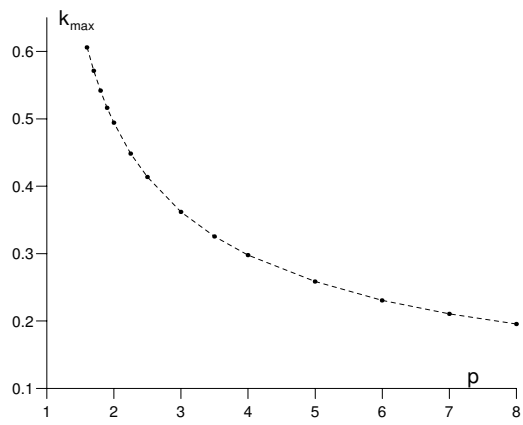
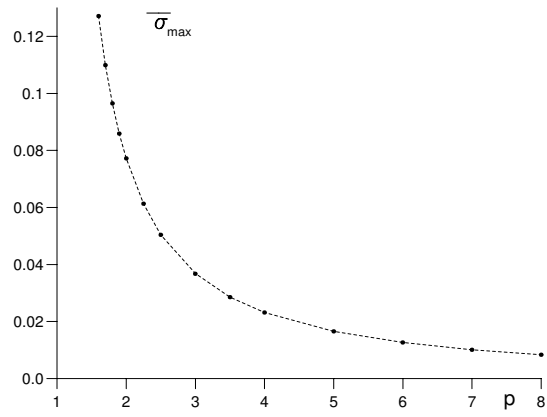
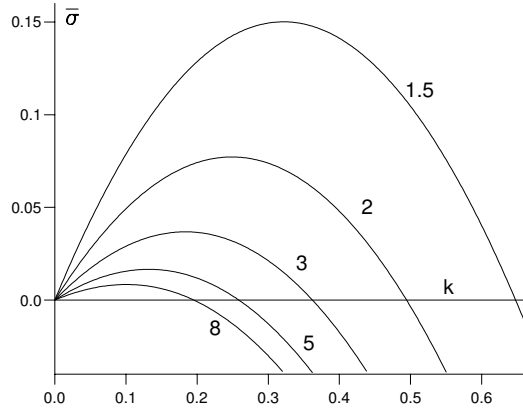


Figure 8

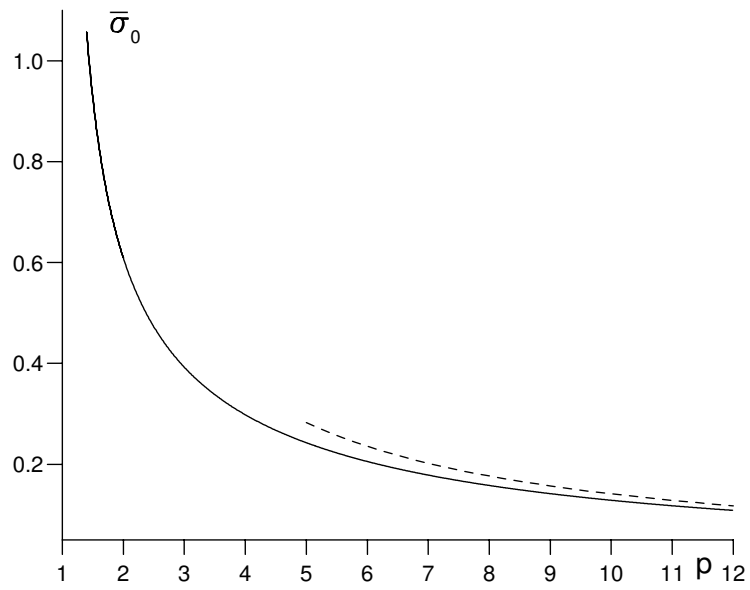


Figure 9